Proposal of Coupling of a Microwave Cavity with a Quartz Resonantor

Ujjawal Singhal

A dissertation submitted for the partial fulfilment of
BS-MS dual degree in Science.

Indian Institute of Science Education and Research Mohali

April 2018

Certificate of Examination

This is to certify that the dissertation titled **"Proposal of Coupling of a Microwave Cavity with a Quartz Resonator"** submitted by **Mr. Ujjawal Singhal** (Reg. No. MS13055) for the partial fulfillment of BS-MS dual degree programme of the Indian Institute of Science Education and Research, has been examined by the thesis committee duly appointed by the Institute. The committee finds the work done by the candidate satisfactory and recommends that the report be accepted.

Prof. Sudeshna Sinha	Dr. Sandeep Goyal	Dr. Ananth Venkatesan
		(Supervisor)

Dated : April 20, 2018

Declaration

The work presented in this dissertation has been carried out by me under the guidance of Dr. Ananth Venkatesan at the Indian Institute of Science Education and Research Mohali.

This work has not been submitted in part or in full for a degree, a diploma, or a fellowship to any other university or institute. Whenever contributions of others are involved, every effort is made to indicate this clearly, with due acknowledgment of collaborative research and discussions. This thesis is a bonafide record of original work done by me and all sources listed within have been detailed in the bibliography.

Ujjawal Singhal

(Reg. No. MS13055)

Dated: April 20, 2018

In my capacity as the supervisor of the candidate's project work, I certify that the above statements by the candidate are true to the best of my knowledge.

Dr. Ananth Venkatesan

(Thesis Supervisor)

Acknowledgement

I would like to express my sincere gratitude to my supervisor Dr. Ananth Venkatesan, Department of Physical Sciences, IISER Mohali for his continuous support, invaluable guidance and encouragement during the entire course of this MS thesis project work. I am thankful to him for his helpful nature and willingness to answer all my queries.

I would also like to thank the other thesis committee members for their suggestions and comments. A special thanks goes to Prof. Jasjeet Singh Bagla and Dr. Mandip Singh for providing me with the magnetic field setup that I have used in this thesis work.

I would like to take this opportunity to thank the PhD scholars of the Ultra Low Temperature Physics Lab, Shailender Kumar and Shyamsundar Yadav for making me feel comfortable in the lab and helping me with the working of various instruments.

I must express my very profound gratitude to my parents and to my friends for their constant support and continuous encouragement. This thesis would not have been possile without them.

Contents

List of Figures

Chapter 1

Introduction

In this chapter we will describe the basic setups and theory of cavity optomechanics.We will first study the coupled harmonic oscillator in order to understand the splitting of normal modes. So that later we can relate the the optomechanical setup with the coupled harmonic oscillator.

1.1 A classical Mechanical Harmonic Oscillator

The harmonic oscillator is a basic textbook example of classical mechanical systems. Mechanical oscillations are a widespread form of motion in nature,for example, it can be found in almost any kind of physical system-from microscopic objects such as molecules up to the biggest found in our universe including neutron stars or more familiarly in systems like clocks, engines or musical instruments. The concept is always the same: an oscillation is the repetitive variation of some parameter around a central value. For example, a system at an initial position x_0 experiences a restoring force F that is proportional to its position x, returns to its point of origin and subsequently moves back to x_0. As long as the system stays decoupled from its environment it continues with this oscillatory movement. According to Newton's second law, the system is described by $F = m\ddot{x} = -kx$,where F is a force, m is the mass of the harmonic oscillator, $\ddot{x}$ is the second derivative of its position with respect to time and k is a positive constant, usually referred to as the spring constant. This is a simple differential equation and one easily sees that the equation of motion is given by

$$x(t) = A\sin(\omega_m t + \psi)$$

Here A is the amplitude, which is determined by the initial conditions and $w_m = 2\pi f_m$ is the oscillator's eigenfrequency. The phase ψ is the position of the oscillator relative to the point of origin at t = 0 and is also determined by the initial conditions. In fact A and ψ are given by[1]

$$A = \sqrt{\dot{x}^2/\omega_m + x^2},$$

$$\psi = arctan(\omega_m x(0)/\dot{x}(0))$$

Eigenfrequency of the system is

$$\omega_m = 2\pi/\tau_m = \sqrt{k/m}$$

where τ_m is the period of oscillation.The total energy E_tot of the harmonic oscillator is conserved, only it total kinetic energy E_{kin} and total potential E_{pot} vary with time as,

$$E_{kin} = (m/2)\dot{x}^2 = (k/2)A^2cos^2(\omega_m t + \psi)$$

$$E_{pot} = (k/2)x^2 = (k/2)A^2 sin^2(\omega_m t + \psi),$$

Now the total energy is given by,

$$E_{tot} = E_{kin} + E_{pot} = (m/2)\omega_m^2 A^2$$

The aboves mentioned equations are for free harmonic oscillator, but the real harmonic oscillator experiences some kind of friction as it interacts with it's environment and therefore we have to include damping in the equation of motion. Therefore the equation which includes damping is given by

$$\ddot{x} + \Gamma_m \dot{x} + {\omega_m}^2 x = 0$$

Here Γ_m is the damping rate and it tells about, how fast the oscillations decays.Now the solution of the damped harmonic oscillator is given by [1]

$$x(t) = A_d e^{-\Gamma_m/2t} sin[\sqrt{{\omega_m}^2 - (\Gamma_m/2)^2 t} + \psi_d]$$

Where A_d and ψ_d are the amplitude and phase of the damped harmonic oscillator respectively. Now there is a very useful quantity for the damped harmonic oscillator is its quality factor Q, which measures how many oscillations it undergoes before it's amplitude decays by a factor of e:

$$Q = \omega_m/\Gamma_m$$

The three different alternatives associated with quality factor are:

1) $Q > 1/2$: In this condition, the system is underdamped. In this condition the oscillator oscillates at a slightly different frequency than the free harmonic oscillator and gradually decays to zero.

2) $Q = 1/2$: In this condition, the system is critically damped. In this condition the oscillator attempts to return to its equilibrium position as quickly as possible and does this without oscillating at all.

3) $Q < 1/2$: In this condition, the system is overdamped. In this condition the oscillator oscillator also returns to its equilibrium position without oscillations but takes longer than in the critically damped case – the smaller Q becomes, the longer it takes.

Now the real harmonic oscillator is not only damped but it is also coupled with the external bath(surrounding) that drives it's motion. The equation of such damped and driven harmonic oscillator s given by:

$$\ddot{x} + \Gamma_m \dot{x} + {\omega_m}^2 = F(t)/m,$$

where F(t) in the simplest case is a harmonic driving force of the form F(t) = F_0 sin(ωt) but can in general take the form of any arbitrary external force. We can again take an Ansatz of the form x(t) = A sin(ωt + ψ) and we can get the amplitude relation and the phase relation respectively as:

$$A = (F_0/m)/\sqrt{({\omega_m}^2 - \omega^2)^2 + \omega^2 {\Gamma_m}^2},$$

$$\psi = arctan((-\omega\Gamma_m)/({\omega_m}^2 - \omega^2)^2),$$

The response of the damped, driven harmonic oscillator is similar to a Lorentzian and has its resonance close to the natural frequency of the oscillator. It is given by

$$\omega_{res} = \omega_m \sqrt{1 - {\Gamma_m}^2/2{\omega_m}^2},$$

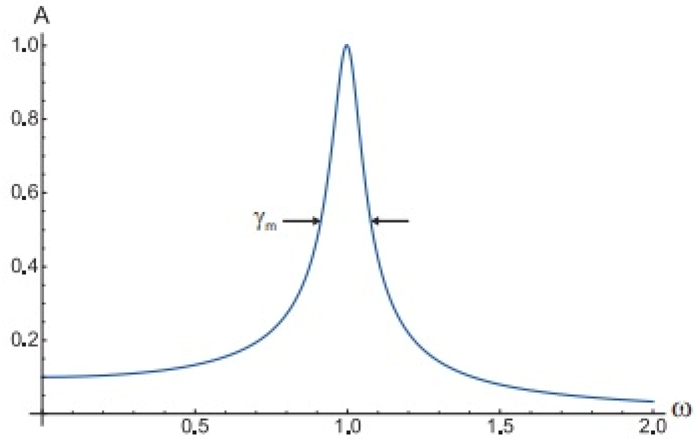

FIGURE 1.1: The amplitude response A of a damped, driven harmonic oscillator as a function of frequency ω . In this example the unperturbed frequency ω_m = 1 and the damping $\Gamma_m = 0.1\omega_m$, which is defined as the full width at half maximum (FWHM) of the resonance.(ref:simon grblacher thesis)

1.2 Normal modes of coupled harmonic oscillator

An interesting effect occurs if two harmonic oscillators are coupled together (fig 1.2)) – for sufficiently strong coupling the two oscillators can be described as one single system oscillating at frequencies that are determined by their coupling strength. The differential equations for two simple harmonic oscillators that are coupled by a spring with spring constant k_j are

$$m\ddot{x}_1 = -kx_1 + k_j(x_2 - x_1),$$

$$m\ddot{x}_2 = -kx_2 + k_j(x_1 - x_2),$$

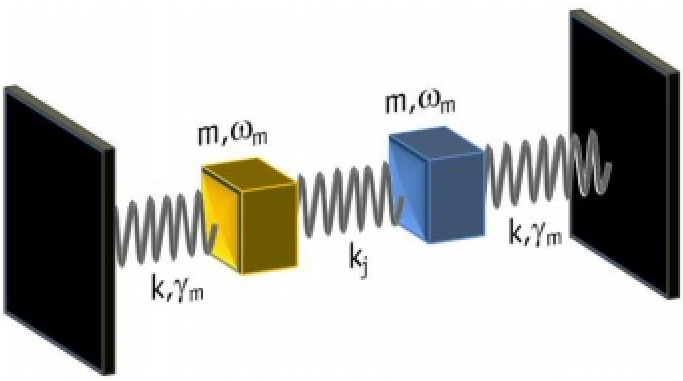

FIGURE 1.2: Coupled harmonic oscillators. Above Two oscillators have same masses m and frequencies ω_m are each coupled to an environment via a spring with a spring constant k and a damping rate Γ_m. In addition, they are coupled to each other via a joint spring with a spring constant k_j.(ref:simon grblacher thesis)

For simplicity, here the oscillators have the same mass m and spring constant k. Taking the Ansatz x_1(t) = Asin(ωt+ ψ) and x_2(t) = Bsin(ωt+ ψ) and substituting the above ansaltz solutions[2] in the coupled differential equations we find

$$(k + k_j - m\omega^2)A - k_j B = 0,$$

$$-k_j A + (k + k_j - m\omega^2)B = 0,$$

For the equation to have a non-trivial solution the determinant of the system of equations must be singular, i.e. zero:

$$(k + k_j - m\omega^2)^2 - {k_j}^2 = 0,$$

This is a simple quadratic equation in ω and assuming that $\omega \geq 0$ we obtain

$$\omega_1 = \sqrt{(k + 2k_j)/m},$$

$$\omega_2 = \sqrt{k/m},$$

Now subsituting back these in coupled amplitudes equations, we get $A = B \equiv A_1$ and $A = -B \equiv A_2$ for the two frequencies respectively. The most general equations of motions now are

$$x_1(t) = A_1 \sin(\omega_1 t + \psi_1) + A_2 \sin(\omega_2 t + \psi_2),$$

$$x_2(t) = -A_1 \sin(\omega_1 t + \psi_1) + A_2 \sin(\omega_2 t + \psi_2),$$

The amplitudes $A_{1,2}$ and the phases $\psi_{1,2}$ are determined by the initial conditions of $x_{1,2}$(0) and $\dot{x}_{1,2}$(0). The motion of the oscillators can therefore be decomposed into two normal modes with frequencies $\omega_{1,2}$ and amplitudes $A_{1,2}$, which are nondegenerate for $k_j \neq 0$.

The system becomes even more interesting for two damped (and driven) oscillators. Their uncoupled equations of motions are given by

$$\ddot{x}_1 + \Gamma_m \dot{x}_1 + {\omega_m}^2 x_1 - (k_j/m)(x_2 - x_1) = 0,$$

$$\ddot{x}_2 + \Gamma_m \dot{x}_2 + {\omega_m}^2 x_2 - (k_j/m)(x_1 - x_2) = F(t)/m$$

Here we assumed that Γ_m , ω_m, m of both the oscillators are same and one oscillator is driven by external force F(t). The solutions of above equations are

$$q_1(t) = A_1 \sin(\omega_m + \psi_1)$$

$$q_2(t) = A_2 \sin(\omega_m + \psi_2)$$

where q_1 and q_2 are the normal modes coordinates with $q_1 = x_1 + x_2$ and $q_2 = x_2 - x_1$. Therefore the frequency of normal modes are give by

$$\omega_1 = \sqrt{(k + 2k_j)/(m - ({\Gamma_m}^2/4))},$$

$$\omega_2 = \sqrt{k/(m - ({\Gamma_m}^2/4))},$$

and there respective amplitudes are given by

$$A_i = (F_0/m)/\sqrt{({\omega_i}^2 - \omega^2)^2 + \omega^2 {\Gamma_m}^2},$$

with i=1,2. Now if we see the spectrum of the normal modes(as shown in figure 1.3), it is seen that the modes are degenerate as long as long as the coupling strength between the oscillators is small ie. $k_j << \gamma_m$. Here we can see that normal modes are only degenerate only if coupling strength between them is greater than the damping with the environment.

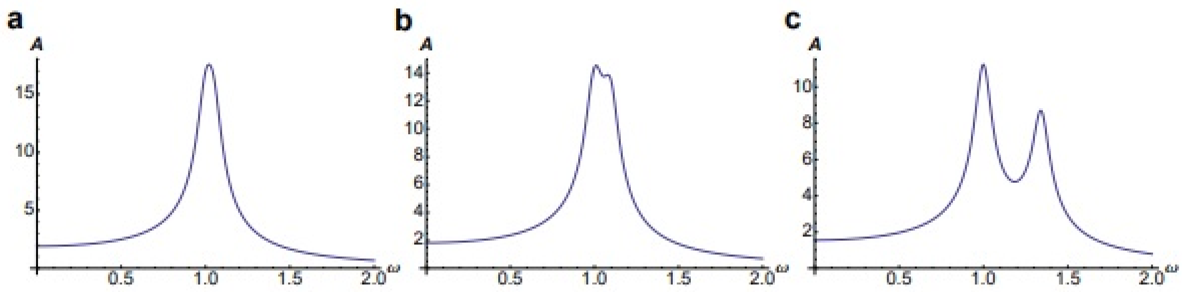

FIGURE 1.3: Splitting of normal modes in damped coupled harmonic oscillators. The spectrum of two coupled oscillators is shown for different coupling constants k_j . The parameters of the oscillators are chosen to be $F(t) = m = k = \omega_m = 1$ and $\Gamma_m = 0.1\omega_m$. a For a coupling $k_j = 0.5\Gamma_m$ the normal modes are still degenerate, while for $k_j = \Gamma_m$ the splitting can already be observed b. c When increasing the coupling further to $k_j = 4\Gamma_m$ the modes become very distinct.

1.3 A quantum mechanical harmonic oscillator

Harmonic oscillator is one of the basic example in quantum mechanics. This system shows some peculiar quantum effects that makes it so distinct from classical mechanics. To understand the quantum nature of harmonic oscillator, we first have to write its hamiltonian. If one replaces the classical variables with their corresponding quantum operators, i.e.$x \rightarrow x$ and m$\dot{x}$ = p = -i$\hbar\frac{d}{dx}$ one obtains the quantum mechanical Hamiltonian operator

$$H = -\frac{\hbar^2}{2m}\frac{d^2}{dx^2} + \frac{m\omega^2 x^2}{2},$$

Now we can write position and momentum operators in terms of creation and annihilation operators.

$$x = \sqrt{\frac{\hbar}{2m\omega}}(a + a^\dagger),$$

$$p = \sqrt{\frac{m\omega\hbar}{2}}(a - a^\dagger).$$

Here x,p,a and $a^\dagger$ satisfy the following commutation relations [x,p] = i$\hbar$, [a,$a^\dagger$] = 1, [a,a] = [$a^\dagger$,$a^\dagger$] = 0

Hence the Hamiltonian can now be written as

$$H = \hbar\omega(a^\dagger a + \tfrac{1}{2}),$$

and now the schrodinger equation can be written as

$$a^\dagger a\psi = (\frac{E}{\hbar\omega} - \frac{1}{2})\psi,$$

Now we can write the ground state wavefunction ψ_0 for the harmonic oscillator, this we can calculate using aψ = 0, and can be written as

$$\psi_0(x) = (\frac{m\omega}{2\hbar})^{\frac{1}{4}}\exp^{\frac{-m\omega^2 x^2}{2\hbar}},$$

The wavefunction of excited states can be written as

$$\psi_n(x) = (\tfrac{1}{n!})^{\frac{1}{2}}(a^\dagger)^n\psi_0(x),$$

It is now easy to find the energy spectrum for the harmonic oscillator by simply writing down the eigenvalue equation for the Hamiltonian, which is discrete and the energy levels are equidistant:

$$E_n = \hbar\omega(n + \tfrac{1}{2}),$$

Now we can calculate the expectation value of position operator and the square of position operator.Therefore

$$< x >=< \psi_n|x|\psi_n >= 0,$$

$$< x^2 >=< \psi_n|x^2|\psi_n >= \tfrac{\hbar}{m\omega}(n + \tfrac{1}{2},$$

From the above equation we can see that the ground state of harmonic oscillator has non zero energy,which is given by $E_0 = \frac{\hbar\omega}{2}$ Now due to this non zero ground state energy, there is uncertainity in the position of the ground state, which is called zero point extension and is given by

$$x_{zp} = \sqrt{< x^2 >_0 - < x_0 >^2} = \sqrt{\tfrac{\hbar}{2m\omega}},$$

One point to note from above equation is that if the frequency or mass of the oscillator increases than the zero point extension decreases.

1.4 Radiation pressure

Electromagnetic radiation exerts a force on everything it encounters.Due to which the object feels a minute pressure upon itself.This is known as radiation pressure[3,4], and can be thought of as the transfer of momentum from photons as they strike the surface of the object.The effects of radiation pressure have been discussed as early as the 17th century when Johannes Kepler suspected that the inclination of tail of comets could be due to a mechanical force exerted by the sun[5,6]. In the early 20th century, experiments Lebedev [7] and Nichols and Hull [8] first verified unambiguously predictions by Maxwell [9] and Bartoli [10] on the strength of the radiation-pressure force. In the 1960s and 70s, Braginsky and colleagues studied radiation-pressure effects in the context of gravitational wave antennae – they experimentally and theoretically analyzed the sensitivity limits due to the quantum nature of light [11, 12]. . First experiments on radiation-pressure effects in cavities with macroscopic mechanical oscillators were performed in the 1980s [13]. Subsequently, several theoretical proposals for quantum optics experiments in a cavity using radiation-pressure effects were published, such as the generation of squeezed light [14, 15], quantum non-demolition measurements of photon numbers [16, 17], feedback-cooling of the mechanical motion [18] (which was experimentally realized in [19]), entanglement between the optical and the mechanical mode [20–22], and the quantum-state transfer from the light field to the mechanical oscillator [23]. However, first experiments were only realized in recent years (except for [23]): measurements of the motion of a mechanical oscillator [24–26], parametric amplification of the mechanical motion [27], cavity cooling of the mechanical resonator [28–31], cryogenic cavity cooling [32–35] and strongly coupled opto-mechanics [36]. . It is important to note that experiments involving nanomechanical oscillators and microwave cavities have achieved similar results[37,38].

1.5 Cavity Optomechanics

Cavity optomechanics as the name suggests, is basically the interaction between light(electromagnetic field mode) and the mechanical object.In optomechanics a cavity play a important role, because using cavity we can trap the light in order to maximize the effect of radiation pressure force on mechanical object. The basic set-up of cavity optomechanics is a Fabry-Perot cavity, in which one of the end-mirrors is suspended, i.e. it can be described as a damped harmonic oscillator with a resonance frequency ω_m and a mass m, subject to an external thermal bath and coupled to the light inside the cavity via the radiation-pressure force as shown in figure(1.4).

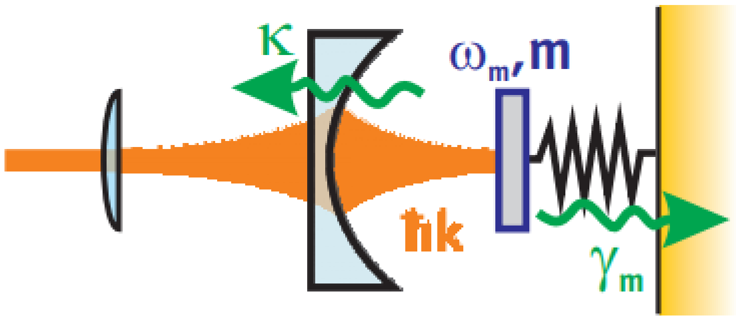

FIGURE 1.4: Basic set-up of the radiation-pressure interaction: light is coupled through a rigid input mirror into an optical resonator with a movable back-mirror of frequency ω_m and mass m. The photons inside the cavity each transfer momentum of $2\hbar\kappa$ onto the movable mirror, displace it and hence acquire a phase shift, depending on its position. The intensity of the light field inside the cavity strongly depends on the relative distance between the mirrors, as well as on their reflectivities – the amplitude cavity decay rate is given by κ. The movable mirror couples to its environment at a rate Γ_m.

1.6 Various Optomechanical setups

There are various optomechanical setups which shows the same radiation pressure effect as discussed in section(1.4).In figure(1.5) there are two optomechanical systems. The first system is same as the fabry perot setup and the second system is also a type of optomechanical system. In the second system you can see a LC circuit which is inductively coupled to a microwave drive. In this circuit the distance between the plates of the capacitor varies due to which the resonance frequency of Lc circuit changes.

1.6.1 Hamiltonian of optomechanical system

Here we will describe the basic hamiltonian of optomechanical systems[4]. Here we will consider a simple febry perot cavity in order to derive the hamiltonian. Suppose we have uncoupled cavity with resonance frequency w_{cav} and a uncoupled mechanical resonator with resonance frequency ω_m. Now you can think of a cavity and mechanical resonator as two harmonic oscillator. Therefore the basic hamiltonian becomes

$$\hat{H}_0 = \hbar w_c av \hat{a}^\dagger \hat{a} + \hbar\omega_m \hat{b}^\dagger \hat{b},$$

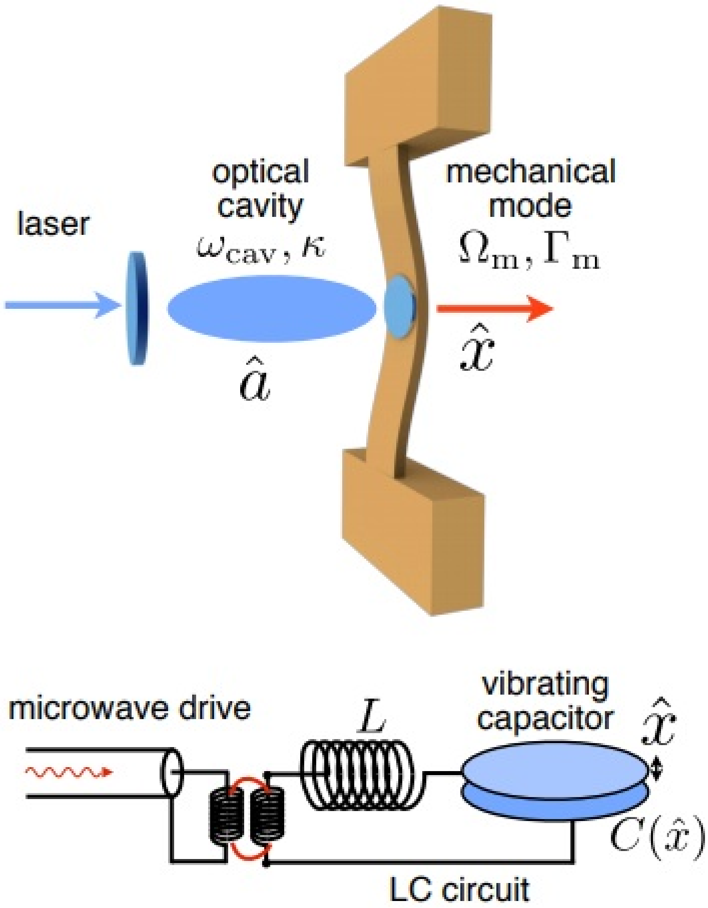

FIGURE 1.5: Schematic of a generic optomechanical system, both in the optical domain (top), with a laser-driven optical cavity and a vibrating end mirror, as well as in the microwave domain (bottom), with a vibrating capacitor. Here we have depicted a microwave drive entering along a transmission line that is inductively coupled to the LC circuit representing the microwave resonator.(ref:[4]

where $\hat{a}^\dagger$ $(\hat{a})$ are the creation(annihilation) operators of photons and $\hat{b}^\dagger$ $(\hat{b})$ re the creation(annihilation) operators of phonons. Now in the case of cavity with a movable mirror, as the mirror moves the length of cavity changes due to which the cavity resonance frequency gets modulated(resonance frequency becomes the function of distance),

$$w_{cav}(x) \approx w_{cav} + x\frac{\partial w_{cav}}{\partial x} + ...$$

we can also write it as

$$w_{cav}(x) \approx w_{cav} - Gx + ...$$

where we define the optical frequency shift per displacement as $G = -\frac{\partial w_{cav}}{\partial x}$ For a simple cavity of length L, we have $G = \frac{w_{cav}}{L}$ The sign reflects the fact that we take x > 0 to indicate an increase in cavity length, leading to a decrease in $w_c av(x)$ if G > 0. In general, expanding to leading order in the displacement, we have:

$$\hbar w_{cav}(x)\hat{a}^\dagger\hat{a} \approx \hbar(w_{cav} - G\hat{x})\hat{a}^\dagger\hat{a}$$

Here $\hat{x} = x_{zp}(\hat{b} + \hat{b}^\dagger)$. Therefore interaction part of hamiltonian may be written as

$$\hat{H}_{int} = -\hbar g_0 \hat{a}^\dagger \hat{a}(\hat{b} + \hat{b}^\dagger)$$

where

$$g_0 = G x_{zp}$$

is the vacuum optomechanical coupling strength, expressed as a frequency. It quantifies the interaction between a single phonon and a single photon.The Hamiltonian reveals that the interaction of a movable mirror with the radiation field is fundamentally a nonlinear process, involving three operators (three wave mixing).The radiation pressure force is simply the derivative of $\hat{H}_{int}$ with respect to displacement:

$$\hat{F} = -\frac{d\hat{H}_{int}}{d\hat{x}} = \hbar G \hat{a}^\dagger \hat{a} = \hbar \frac{g_0}{x_{zp}} \hat{a}^\dagger \hat{a}$$

1.7 Sidebands due to optomechanical interaction

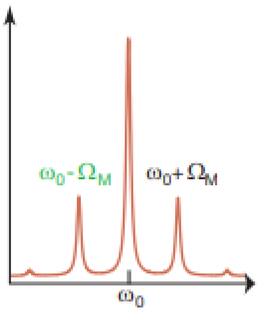

FIGURE 1.6: Sidebands appears due to optomechanical interaction.(ref: o colonel thesis)

In figure(1.6) there are 3 peaks shown, in which the central peak is due to the cavity resonance and right and left peaks are anti-stokes and stokes respectively. Where stokes and anti-stokes bands corresponds to the transfer of photons from laser to mechanical mode and vice versa. In section 1.1 we learned that the normal mode splitting of two harmonic oscillator takes place only when the coupling spring constant is greater than the damping rate. Therefore we can consider cavity and mechanical oscillator as two harmonic oscillator which are coupled to each other through a constant g. We briefly note that g > κ is one neccessary condition for the so-called "strong coupling" regime of cavity optomechanics, where the mechanical oscillator and the driven optical mode hybridize.A much more challenging condition is to have $g_0 > \kappa$, i.e. the single photon optomechanical coupling rate exceeding the cavity decay rate. In order to cool the mechanical oscillator, the system should be in sideband resolved-regime ($\kappa << \omega_m$) Where g referred to as optomechanical coupling strength and g_0 is the single photon coupling

$$g = g_0 \sqrt{\bar{n}_{cav}}$$

1.8 Experimental realisations and optomechanical parameter

In order to get the maximum coupling, we need to combine high Q optical resonators with the high Q mechanical oscillator in order to get the maximum optomechanical effect. Therefore we will now discuss some of the optomechanical parameters that effect the optomechanical coupling. Figure(1.7) shows the various type of optomechanical systems that had been used by various research groups in order to study the optomechanical effect.

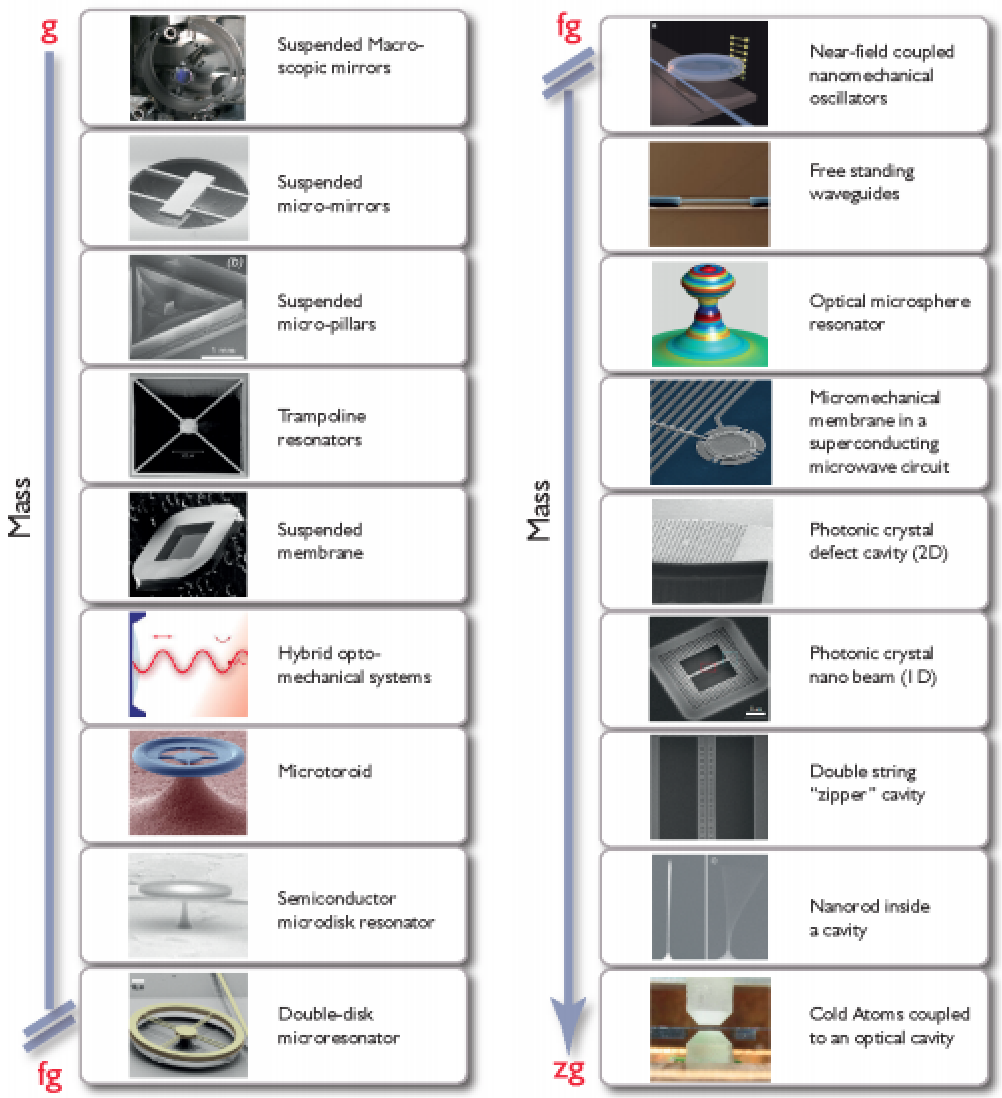

FIGURE 1.7: Various optomechanical devices[4], arranged according to there masses.(ref:[4])

1.8.1 Optomechanical parameters

The following table summarizes the optomechanical parameters for some for the past years experiments.s. These are: the mechanical resonator frequency ω_m and mass m; the fundamental mechanical (phonon) and optical (photon) dissipation rates $\gamma_m = \frac{\omega_m}{Q_m}$ and κ, respectively; the QF product, which is a direct measure for the degree of decoupling from the thermal environment specifically, $Q_m f = Q_m \frac{\omega_m}{2\pi} > \frac{k_b T}{\hbar}$ is the condition for neglecting thermal decoherence over one mechanical period; the sideband suppression factor $\frac{\kappa}{\omega_m}$ that determines the ability to realize ground-state cooling ; and finally the bare optomechanical coupling rate g.

Reference	$\Omega_m/2\pi$[Hz]	m [kg]	$\Gamma_m/2\pi$[Hz]	$Q \cdot f$ [Hz]	$\kappa/2\pi$[Hz]	$\frac{\kappa}{\Omega_m}$	$g_0/2\pi$[Hz]
(Murch *et al.*, 2008)	$4.2 \cdot 10^4$	$1 \cdot 10^{-22}$	$1 \cdot 10^3$	$1.7 \cdot 10^6$	$6.6 \cdot 10^5$	15.7	$6 \cdot 10^5$
(Chan *et al.*, 2011)	$3.9 \cdot 10^9$	$3.1 \cdot 10^{-16}$	$3.9 \cdot 10^4$	$3.9 \cdot 10^{14}$	$5 \cdot 10^8$	0.13	$9 \cdot 10^5$
(Teufel *et al.*, 2011a)	$1.1 \cdot 10^7$	$4.8 \cdot 10^{-14}$	32	$3.5 \cdot 10^{12}$	$2 \cdot 10^5$	0.02	$2 \cdot 10^2$
(Verhagen *et al.*, 2012)	$7.8 \cdot 10^7$	$1.9 \cdot 10^{-12}$	$3.4 \cdot 10^3$	$1.8 \cdot 10^{12}$	$7.1 \cdot 10^6$	0.09	$3.4 \cdot 10^3$
(Thompson *et al.*, 2008)	$1.3 \cdot 10^5$	$4 \cdot 10^{-11}$	0.12	$1.5 \cdot 10^{11}$	$5 \cdot 10^5$	3.7	$5 \cdot 10^1$
(Kleckner *et al.*, 2011)	$9.7 \cdot 10^3$	$1.1 \cdot 10^{-10}$	$1.3 \cdot 10^{-2}$	$9 \cdot 10^9$	$4.7 \cdot 10^5$	55	$2.2 \cdot 10^1$
(Gröblacher *et al.*, 2009a)	$9.5 \cdot 10^5$	$1.4 \cdot 10^{-10}$	$1.4 \cdot 10^2$	$6.3 \cdot 10^9$	$2 \cdot 10^5$	0.22	3.9
(Arcizet *et al.*, 2006a)	$8.14 \cdot 10^5$	$1.9 \cdot 10^{-7}$	81	$8.1 \cdot 10^9$	$1 \cdot 10^6$	1.3	1.2
(Cuthbertson *et al.*, 1996)	318	1.85	$2.5 \cdot 10^{-6}$	$4.1 \cdot 10^{10}$	275	0.9	$1.2 \cdot 10^{-3}$

FIGURE 1.8: optomechanical parameters of past experiment done by research groups.(ref:[4])

Chapter 2

Mechanical Resonator

The mechanical resonator that will be studied in this thesis is a 6MHz AT-cut quartz resonator. In this chapter we will study about the quartz resonator and the experiments that lead to achievement of high quality factor of Quartz resonator.

2.1 What is Quartz?

The technical formula is SiO2 and it is composed of two elements, silicon and oxygen. In its amorphous form SiO2 is the major constituent in many rocks and sand. The crystalline form of SiO2 or quartz is relatively abundant in nature, but in the highly pure form required for the manufacture of quartz crystal units, the supply tends to be small.Quartz crystals are an indispensable component of modern electronic technology. They are used to generate frequencies to control and manage virtually all communication systems. They provide the isochronous element in most clocks, watches, computers and microprocessors. The quartz crystal is the product of the phenomenon of piezo-electricity discovered by the Curie brothers in France in 1880.

2.2 Working

Piezoelectricity is a complex subject, involving the advanced concepts of both electricity and mechanics. The word piezo-electricity takes its name from the Greek piezein "to press", which literally means pressure electricity. Certain classes of piezoelectric materials will in general react to any mechanical stresses by producing an electrical charge. In a piezoelectric medium the strain or the displacement depends linearly on both the stress and the field. The converse effect also exists, whereby a mechanical strain is produced in the crystal by a polarising electric field. This is the basic effect which produces the vibration of a quartz crystals.

2.3 Quartz resonator

Quartz resonators consist of a piece of piezoelectric material precisely dimensioned and orientated with respect to the crystallographic axes. This wafer has one or more pairs of conductive electrodes, formed by vacuum evaporation. When an electric field is applied between the electrodes the piezoelectric effect excites the wafer into mechanical vibration. Many different substances have been investigated as possible resonators, but for many years quartz has been the preferred medium for satisfying the needs for precise frequency generation. Compared to other resonators e.g. LC circuits, mechanical resonators, ceramic resonators and single crystal materials, the quartz resonator has proved to be superior by having a unique combination of properties. The material properties of quartz crystal are both extremely stable and highly repeatable. The acoustic loss or internal fraction of quartz is particularly low, which results in a quartz resonator having an extremely high Q-factor. The intrinsic Q of quartz is 107 at 1 MHz. Mounted resonators typically have Q factors ranging from tens of thousands to several hundred thousands, orders of magnitude better than the best LC circuits. The second key property is its frequency stability with respect to temperature variations. Figure(2.1) shows the modes of vibration of quartz.

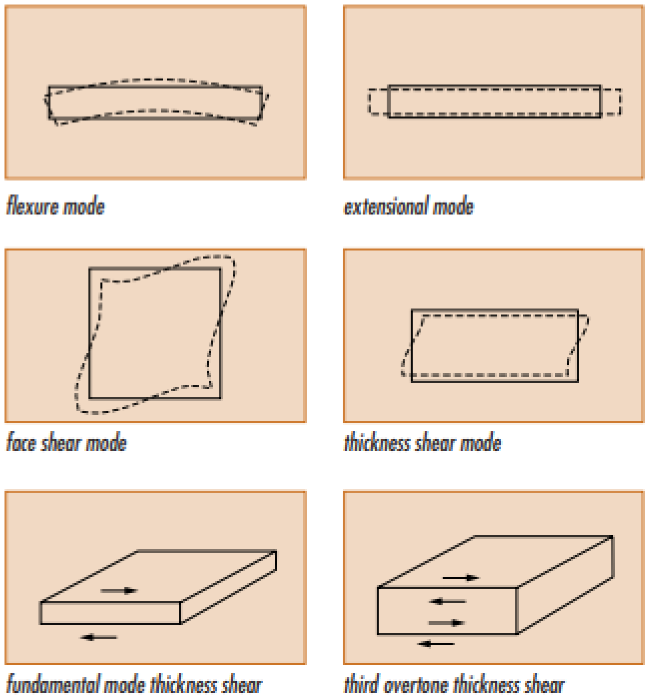

FIGURE 2.1: Modes of vibrations of Quartz resonator.(ref:[40])

2.4 AT-cut Quartz

The AT-cut characteristic (fig.2.2) is the most commonly used type of resonator. It has a frequency temperature coefficient described by a cubic function of temperature, which can be precisely controlled by small variations in the angle of cut. This cubic behaviour is in contrast to most other crystal cuts which give a parabolic temperature characteristic. It makes the AT-cut well suited to applications requiring a high degree of frequency stability over wide temperature ranges. Other important characteristics are aging and quality factor Q.AT cut quartz crystals are widely employed in a range of applications, from oscillators to microbalances[40]. One of the important properties of the AT cut is that the resonant frequency of the crystal is temperature independent to first order. This is desirable in both mass sensing and timing applications. AT cut crystals vibrate in the thickness shear mode—an applied voltage across the faces of the cut produces shear stresses inside the crystal.

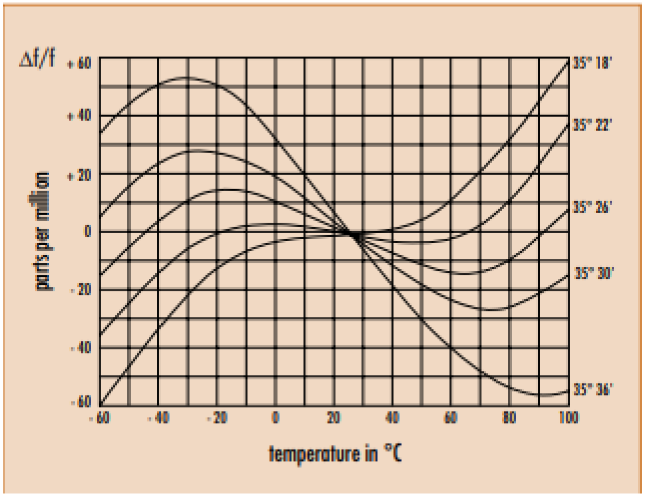

FIGURE 2.2: AT cut frequency temperature curve.(ref:[40])

2.4.1 6MHz AT-cut quartz

This a 1 inch diameter quartz crystal, it has resonance frequency close to 6MHz. It vibrates at a fundamental shear mode at a resonance frequency of 6MHz[41].This thesis uses AT cut quartz, defined in the IEEE 1978 standard as: (YXl) -35.25deg.The first two letters in the bracketed expression always refer to the initial orientation of the thickness (t) and the length (l) of the plate. Subsequent bracketed letters then define up to three rotational axes, which move with the plate as it is rotated. Angles of rotation about these axes are specified after the bracketed expression in the order of the letters, using a right-handed convention. For AT cut quartz only one rotation, about the l axis, is required. In the above figure you can see 2 surfaces of same

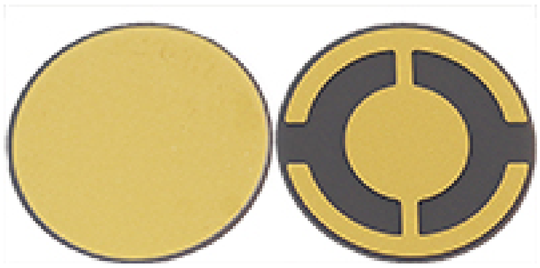

FIGURE 2.3: 6MHz AT-cut quartz.

quartz crystal(one surface is fully covered with gold electrode and other is partially covered.The fully covered surface is convex in shape and other is planar.) Now consider a piezoelectric disc having thickness t, shear mode stress coefficient e_s of the material, shear modulus Y_s, and relative permittivity e_r. One further defines th dimensionless piezoelectric coupling coefficient ${K_0}^2 = \frac{{e_s}^2}{e_r e_0 Y_s}$. A shear deformation by a characteristic distance x corresponds to a shear strain $\lambda_s = x/t$, and generates a piezoelectric surface charge density $\Sigma_q = \lambda_s e_s$. A piezoelectric oscillator is made by metallizing both surfaces of the chip over an area A. The geometric capacitance in the plate-capacitor approximation is then $C_0 = e_r e_0 A/t$. The oscillator can be represent as an equivalent LCR resonator with the effective parameters $C_m = {K_0}^2 C_0, L_m = [(2\pi\omega_m)^2 C_m]^{-1}$ and $R_m = (\omega_m C_m Q)^{-1}$. The corresponding quantised harmonic oscillator xhibits zero-point vibrations of an amplitude $x_{zp} = \sqrt{\frac{\hbar}{2M\omega_m}}$, where M is the effective mass. Figure(2.4,2.5) shows the comsol simulation of 6MHZ AT cut quartz of diameter 14mm.

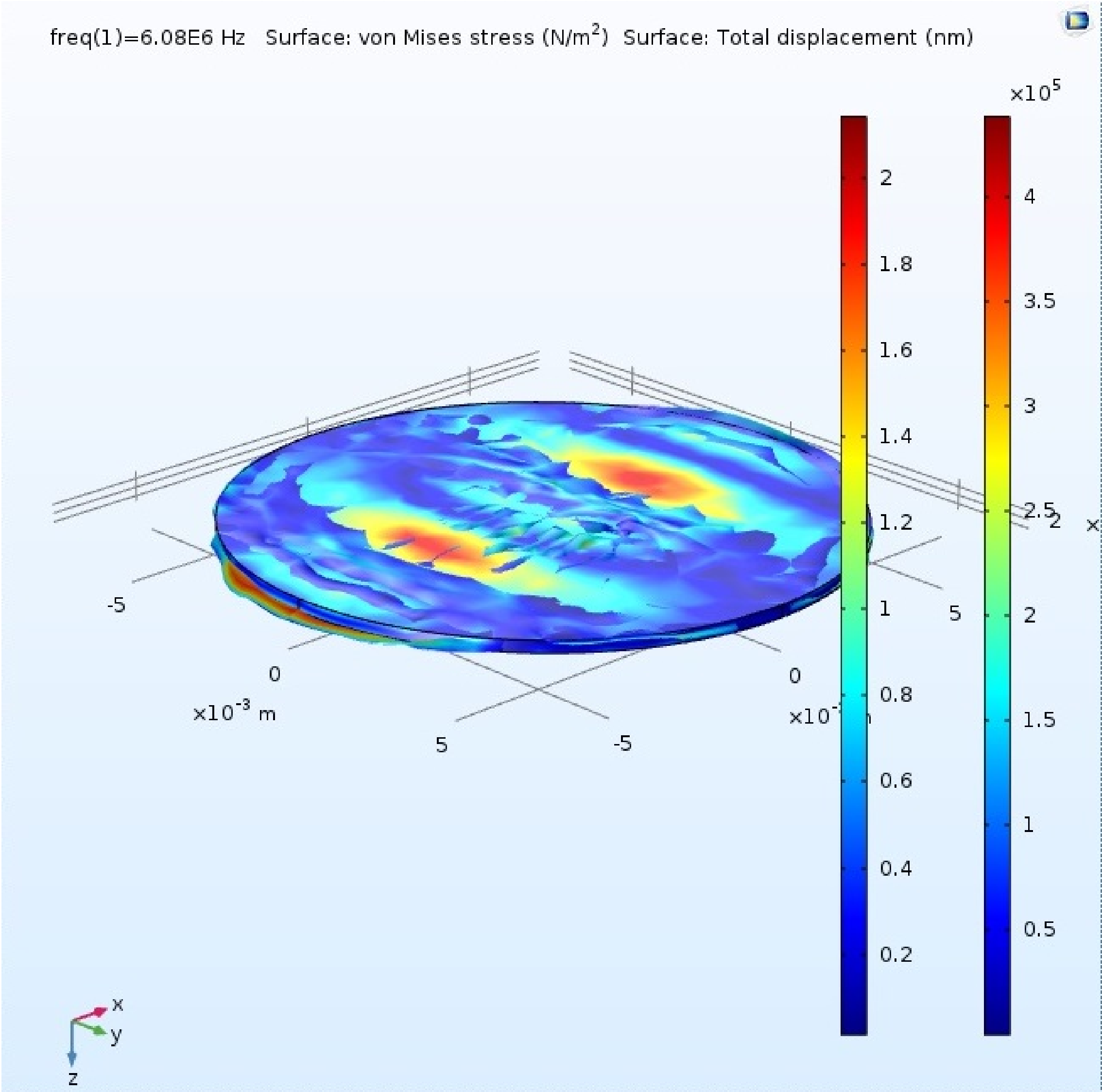

FIGURE 2.4: simulation of stress and displacement of 6MHz AT-cut quartz.

2.5 Recent experiment to increase quality factor of quartz

This experiment was done by the group of people from Aalto university.In this experiment they succeeded in improving the quality factor of quartz using the charge focusing electrode scheme. In this experiment they took 3 quartz among which one is bare quartz, second is quartz coated with aluminium(figure 2.6), third is charge focussing aluminium electrode(figure 2.7). In this experiment they used 6mm diameter, 200μm to 250μm thick plano-convex quartz disks with a fundamental thickness shear mode around 7 MHz. They experimentally measure the dissipation due to

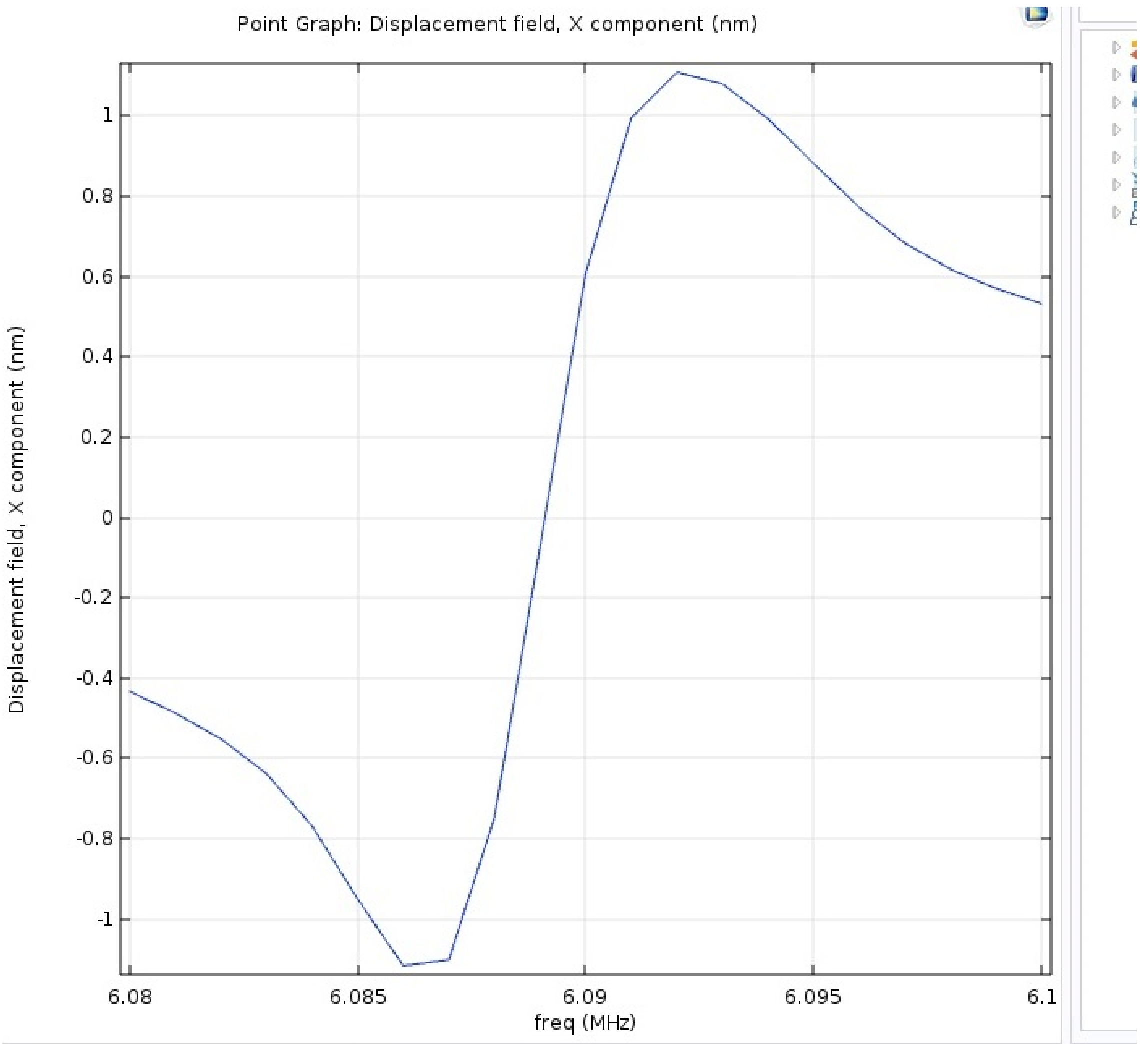

FIGURE 2.5: simulation of displacement vs frequency for 6MHz AT-cut quartz crystal.

charge focusing and thin film electrodes from room temperature down to mk temperatures. In contrast to Ref. [23], they find that dissipation due to uniform thin film electrodes on the quartz surface is negligible, and instead the Q factor is limited by the electrical properties of the grounded charge focusing structures. In the Al-coated quartz electrode configuration there is an Al-island of 2 mm diameter and 30 nm thickness evaporated on the top surface of the piezo disk.

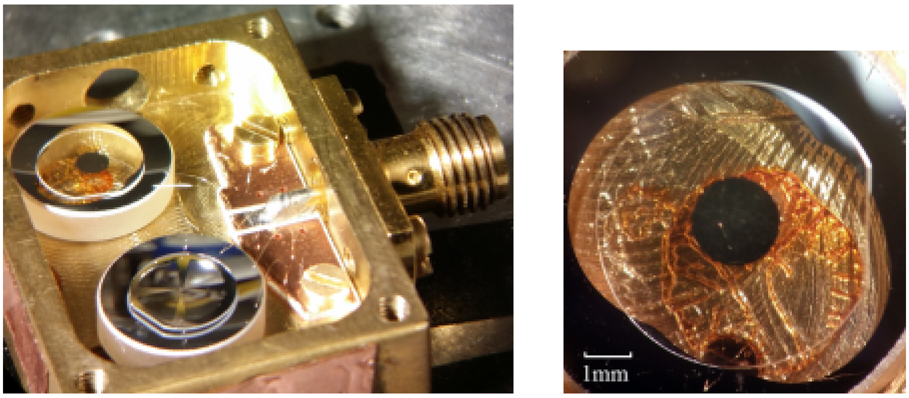

FIGURE 2.6: Photograph of the actuation and transmission measurement setup employed to acquire the resonance frequency and quality factor of the quartz resonator at temperatures ranging from 10 mK to 300 K. Two quartz disk devices are seen laying in lens-shaped supports and Top-view photograph of a quartz disk having an aluminium island (black circle) in the center.(ref:[42])

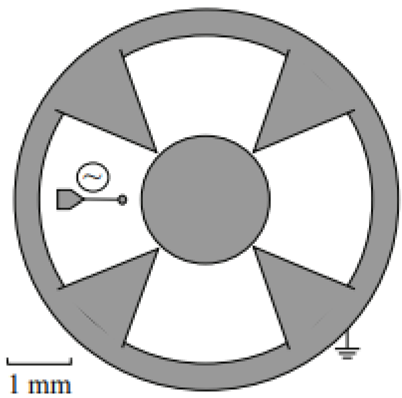

FIGURE 2.7: Charge focussing aluminium electrode.(ref:[42])

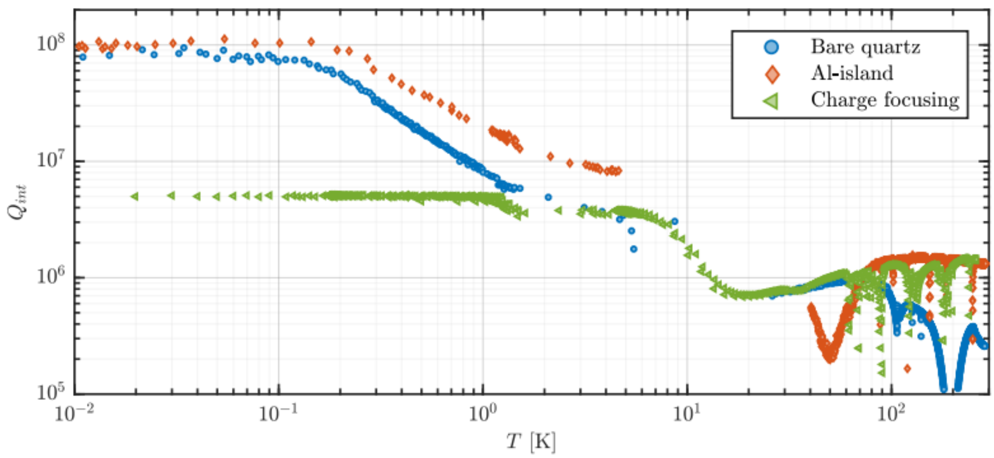

FIGURE 2.8: Dependence of the internal mechanical quality factor on temperature for the three metallization configurations studied in this work: bare quartz disk (blue dots), quartz disk coated with an aluminium thin film island (red diamonds), and quartz disk coated with an aluminium thin film in a charge focusing configuration (green triangles).(ref:[42]

Chapter 3

Experimental design

In this chapter i will describe the design of the experiments that i have done.First one is optomechanical interaction between microwave cavity and quartz resonator. Secondly about the circuit that is used to measure resonance frequency of quartz. Third includes the various experiments that are done to increase quality factor of quartz resonator.

3.1 Coaxial $\lambda/4$ resonator

Quarter-wave ($\Lambda/4$-wave) coaxial resonators[43] are constructed by shorting the center conductor of a coaxial cable to the shield at the far end of the circuit. The length of the cable is exactly $\lambda/4$ at the desired resonant frequency. A short circuit is transformed to an open circuit a quarter wavelength away, so when the $\lambda/4$-wave coaxial resonator is part of an oscillator circuit, it electrically is not even present (Z $\rightarrow \infty$); however, whenever the frequency of the oscillator attempts to go above or below the resonator's center frequency (due to load changes, temperature changes, etc.), the $\lambda/4$-wave section looks like a low impedance that works to attenuate other frequency components.

3.2 Resonant modes

The coaxial transmission line (TL) supports a TEM mode [111] with fields

$$E = \frac{V_0 \exp^{-\gamma z}}{\rho \log ba} \hat{\rho},$$

$$H = \frac{V_0 \exp^{-\gamma z}}{\rho \log ba},$$

The coaxial $\lambda/4$ resonator (Fig. 3.1) is formed by such a TL that is short-circuited on one end and open-circuited on the other by virtue of a narrow circular waveguide. The fundamental resonance frequency f_0, is determined by the length of the transmission line, $l \approx \lambda/4$. We rely on a length L of circular waveguide, located between the $\lambda/4$ section and our light-tight seal, to protect the $\lambda/4$ mode from contact resistance at that joint. Because we design the resonator to be well below the waveguide's cutoff frequency $(f_0 < f_c)$, the fundamental mode's energy density decreases exponentially into the waveguide section, at a rate determined by the radius of the outer conductor.Because the cavity is a $\lambda/4$ resonator, we expect the next transmission line mode at $f_0 \approx 3\lambda/4$. The separation in frequency between the fundamental mode and the next TEM harmonic is actually double the fundamental frequency itself, which provides a remarkably 'clean' spectrum. In fact, waveguide modes of

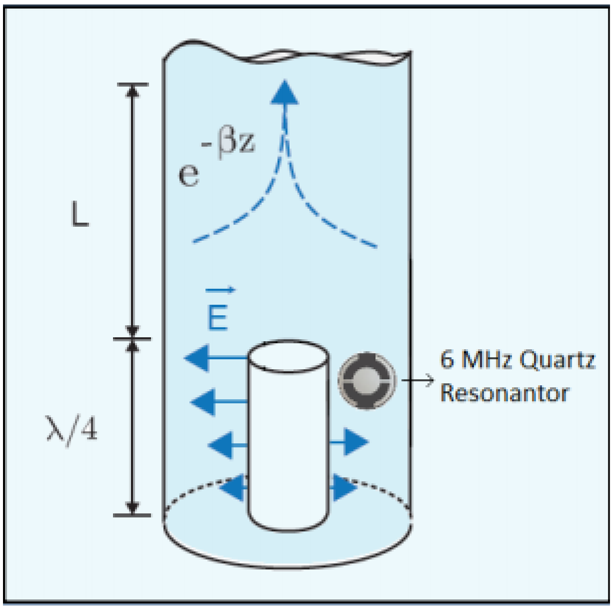

FIGURE 3.1: A quarter-wave coaxial resonator is defined by shorting a coaxial transmission line's inner and outer conductors at one location on the transmission line (bottom) and open-circuiting the line a distance $\lambda/4 away$
and it is coupled with quartz resonator.(ref:[43].

the coax, in particular the TE11 mode, can be lower-lying than the second TEM harmonic. The TE11 mode begins to play a role when $\omega \approx \frac{2c}{(a+b)} = (2\pi)$x15GHz.

In fig.(3.2) you can see the actual setup used in order to couple the cavity and mechanical mode. Here you can see a small cylinder fitted on lid and in front of lid there is a quartz resonator.The cavity is made up of brass Now you can think of this microwave cavity as a parallel LCR circuit, which has a particular resonance frequency. now this cavity has a quartz fitted inside in front of that small cylinder.Now as this quartz vibrate in its lowest shear mode, capacitance of cavity changes and due to which we should get two side bands. Also you can see from fig.(3.1) that the electric field in the cavity is radially outward. Now as this electric field can also interacts with he charge present on surface of quartz. And if we can use the charge focussing scheme than we can enhance this coupling by increasing the charge on the surface of quartz. Fig (3.3) shows the resonance frequency of TEM mode of cavity. Here we have measured s11 parameter in order to find resonance frequency of cavity.Fig.(3.4) shows the comsol simulation of electric and magnetic field inside the microwave cavity. In fig.(3.5) we can see that cavity is having a resonance frequency close to 2.5 GHz. One thing to see from this plot is the cavity linewidth. The cavity linewidth is quite high. That means the losses in the cavity are quite large. In fig.(3.4) you can see the blue and red arrows. Here blue arrows represent the magnetic field and red arrow represents the magnetic field.

3.3 Increasing quality factor of quartz resonator

In this section i will describe the various experiments that i have done in order to increase the quality factor of quartz. In my first experiment first i coat the quartz resonator with 100nm of nickel and measure its response in presence of magnetic

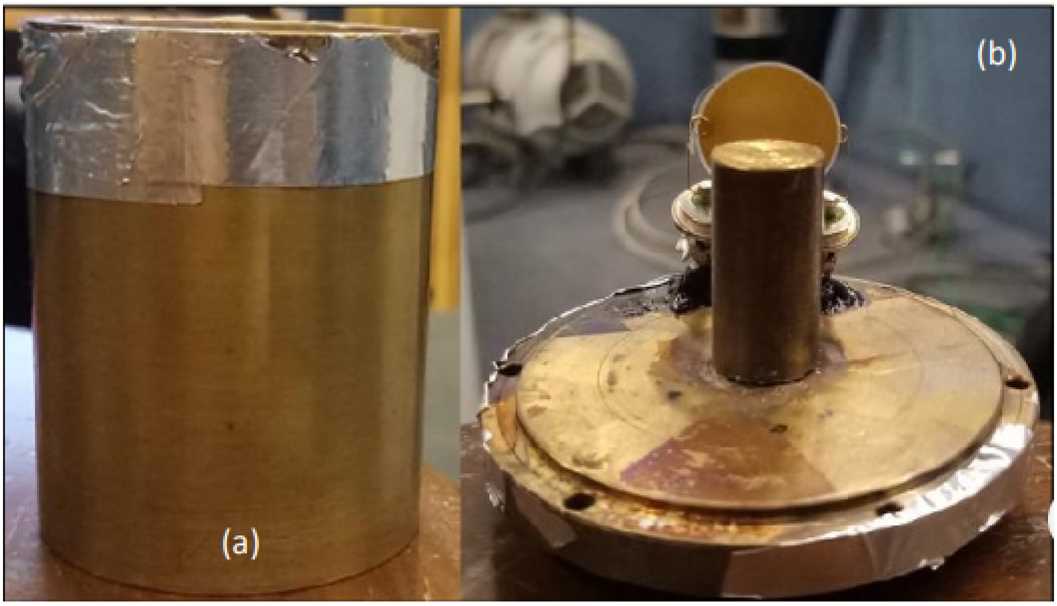

FIGURE 3.2: Setup of cavity fitted with quartz.

field. As nickel is magnetic so the quality factor of nickel coated quartz should be effected by the magnetic field. But in the result it was seen that resonance frequency and quality factor are not enough changing. In my second experiment i coated the quartz with 100nm of Fe-Ni permalloy. And then i measure it response in presence of magnetic field(fig.(3.5)).In this experiment i plot the response of quality factor and resonance frequency for many values of current(ie. magnetic field)

3.4 Quartz cavity

Currently i am also working on a cavity in which quartz is coupled to a magnetic field present inside the cavity and overall it shift the resonance frequency of cavity due to coupling wit the magnetic field.Bic setup is shown in fig(3.6). The design of tunable cavity is based on a typical three-loop, two-gap configuration. The gaps here act as capacitors while the loops act as inductors, so the cavity resonance is analogous to that of an LC circuit. Shown in Fig. 1(b) is a schematic of the cavity. A plunger mounted on a piezoactuator can be moved in and out to change the gap d, which alters the capacitance of the equivalent LC circuit, allowing us to tune the resonance frequency of the cavity.

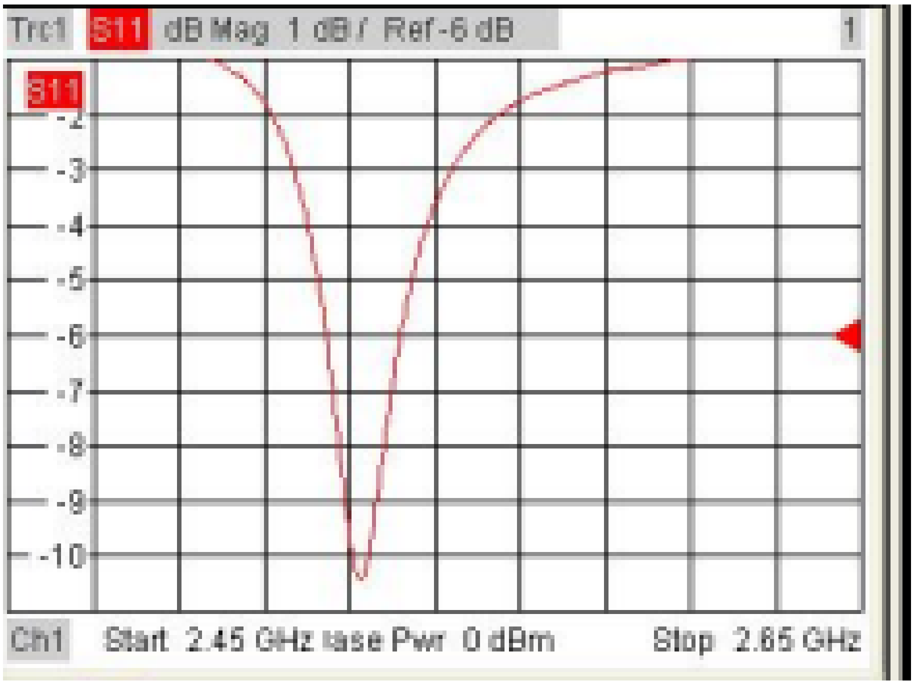

FIGURE 3.3: Resonance frequency response of microwave cavity.

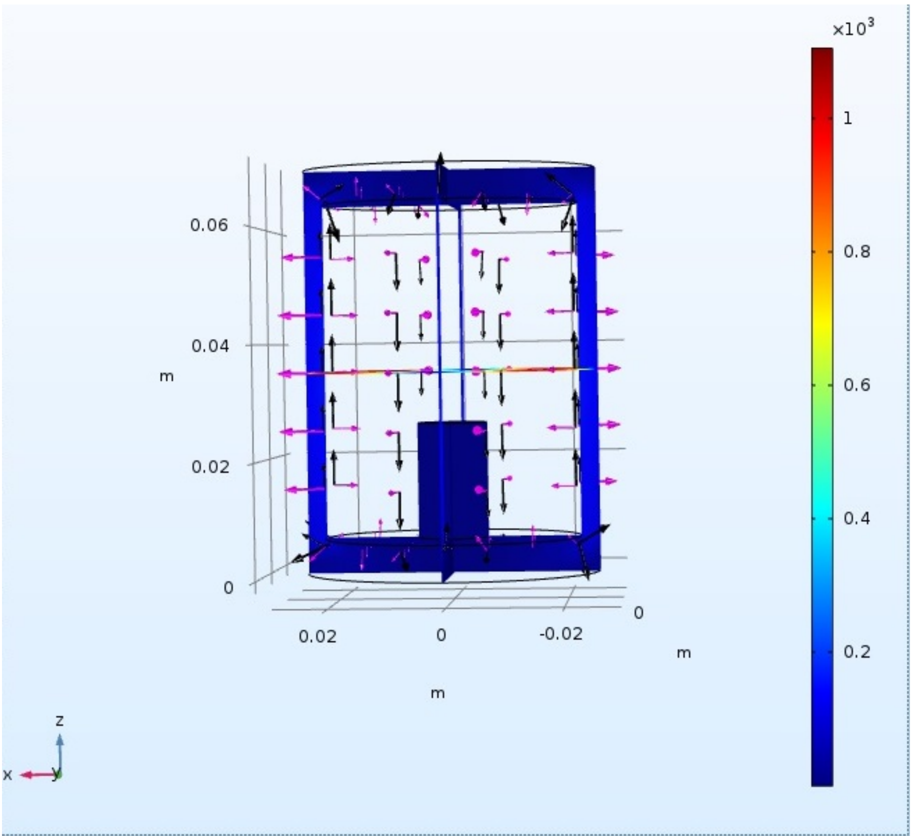

FIGURE 3.4: Comsol simulation of microwave cavity.

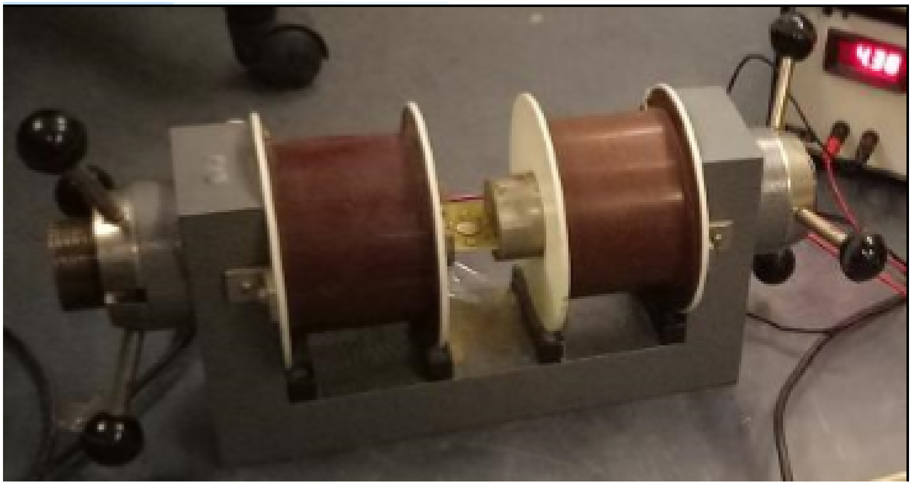

FIGURE 3.5: quartz magnet setup.

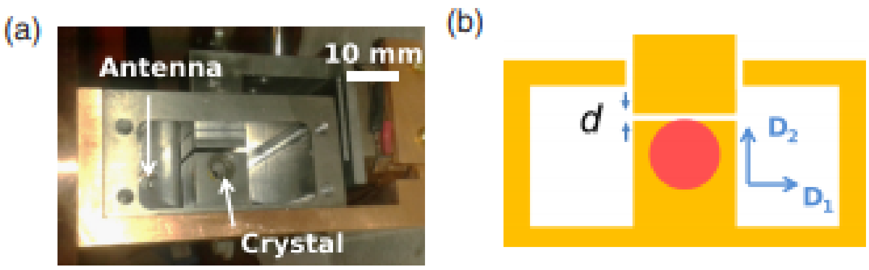

FIGURE 3.6: Two straight antennas are used to couple microwaves in and out. A separated plunger mounted on a piezoactuator is able to move in and out to change the gap size. (b) Schematic picture of the resonator. The resonant frequency can be shifted by changing the gap size d.(ref:[44])

Chapter 4

Conclusion

In this section we will discuss about the results that we have got in doing the previously mentioned experiments. In the first experiment that is to couple the microwave cavity with the quartz resonator. I have not got any coupling between cavity and quartz. This is because the cavity losses in my experiment was dominating over the coupling rate. In order to get this coupling we have to increase the quality factor of both quartz and the microwave cavity so that normal mode splitting condition is satisfied. Other experiment i have tried is to increase the quality factor of quartz. Fig(4.1,4.2) shows the response of quality factor and resonance frequency of quartz in magnetic field. In the above plots we can see that quality factor and

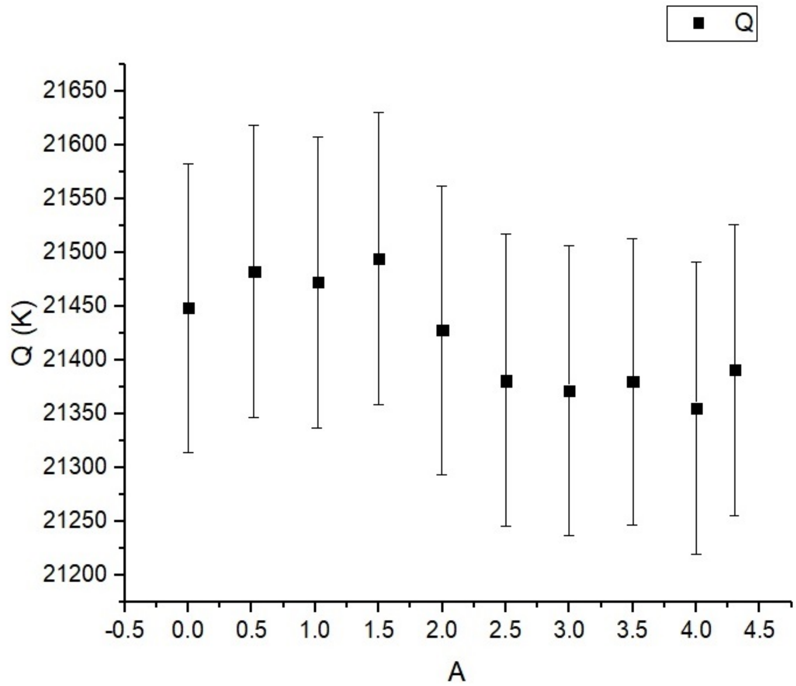

FIGURE 4.1: quality factor vs magnetic field.

resonance frequency are not changing much this my be due to two reasons. First, material deposited on quartz is not enough therefore not much change is seen. Secondly, the maximum current i could send is 4A. Therefore the magnetic may be not enough to cause some noticeable change.

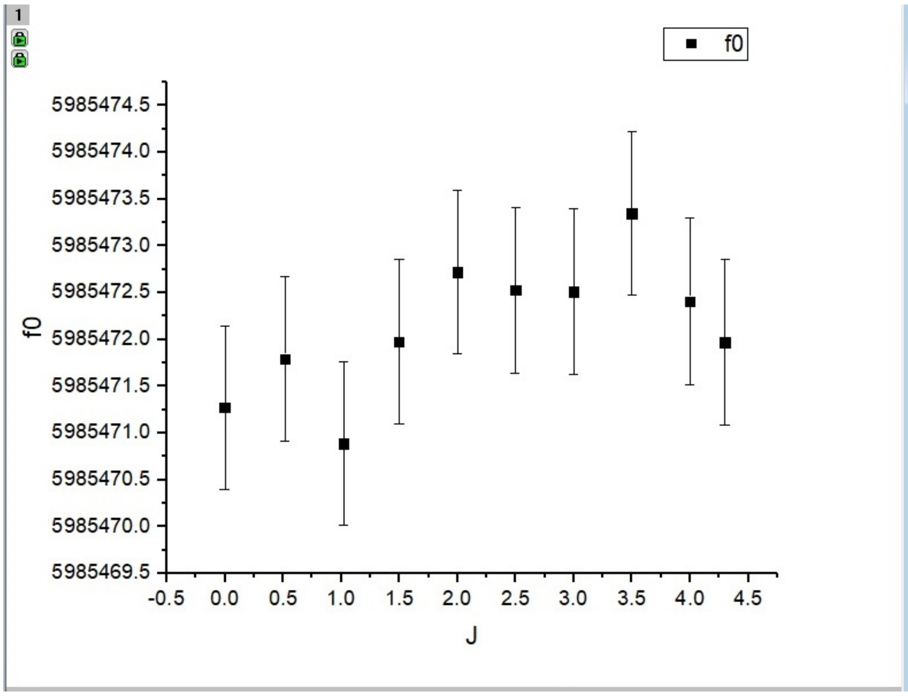

FIGURE 4.2: Resonance frequency vs magnetic field.

Chapter 5

Bibliography

[1] L. Bergmann and C. Schaefer, Lehrbuch der Experimentalphysik: Band 1 - Mechanik, Relativitat, warme (de Gruyter, 1998). 11, 12.
[2] L. D. Landau and E. M. Lifshitz, Mechanics, 3rd edn. (Butterworth- Heinemann, 1976).
[3] Cavity OptomechanicsMarkus Aspelmeyer.
[4] PF Cohadon, A Heidmann, M Pinard - Physical Review Letters, 1999 - APS
[5] J. Kepler, Letter to Galileo Galilei (1610).
[6] J. Kepler, De Cometis Libelli Tres (Augsburg, 1619).
[7] P. Lebedev, Untersuchungen uber die Druckkrafte des Lichtes, Ann. Phys. 6, 433 (1901)
[8] E. F. Nichols and G. F. Hull, About Radiation pressure, Ann. Phys. 12, 225 (1903).
[9] J. C. Maxwell, A treatise on electricity and magnetism, vol. 2 (Clarendon Press, Oxford, 1873).
[10] A. G. Bartoli, Sopra i movimenti prodotti dalla luce e dal calore e sopra il radiometro di Crookes (Le Monnier, Florence, 1876). 21
[11] V. B. Braginsky, Eksp. Teor. Fiz. 53, 1434 (1967). 21
[12] V. B. Braginsky and Y. I. Vorontsov, Quantum-mechanical limitations in macroscopic experiments and modern experimental technique, Sov. Phys. Usp. 17, 644 (1975). 21
[13] V. Braginsky and A. Manukin, Measurement of weak forces in Physics experiments (Univ. of Chicago Press, 1977). 21
[14] C. M. Caves, Quantum-Mechanical Radiation-Pressure Fluctuations in an Interferometer, Phys. Rev. Lett. 45, 75 (1980). 21
[15] P. Meystre, E. M.Wright, J. D. McCullen, and E. Vignes, Theory of radiationpressure-driven interferometers, J. Opt. Soc. Am. B 2, 1830 (1985). 21
[16] A. Dorsel, J. McCullen, P. Meystre, E. Vignes, and H. Walther, Optical Bistability and Mirror Confinement Induced by Radiation Pressure, Phys. Rev. Lett. 51, 1550 (1983). 21
[17] C. Fabre, M. Pinard, S. Bourzeix, A. Heidmann, E. Giacobino, and S. Reynaud, Quantum-noise reduction using a cavity with a movable mirror, Phys. Rev. A 49, 1337 (1994). 21
[18] S. Mancini and P. Tombesi, Quantum noise reduction by radiation pressure, Phys. Rev. A 49, 4055 (1994). 21
[19] K. Jacobs, P. Tombesi, M. J. Collett, and D. F.Walls, Quantum-nondemolition measurement of photon number using radiation pressure, Phys. Rev. A 49, 1961 (1994). 21, 27
[20] M. Pinard, C. Fabre, and A. Heidmann, Quantum-nondemolition measurement of light by a piezoelectric crystal, Phys. Rev. A 51, 2443 (1995). 21, 27
[21] S. Mancini, D. Vitali, and P. Tombesi, Optomechanical Cooling of a Macroscopic Oscillator by Homodyne Feedback, Phys. Rev. Lett. 80, 688 (1998).

[22] P.-F. Cohadon, A. Heidmann, and M. Pinard, Cooling of a Mirror by Radiation Pressure, Phys. Rev. Lett. 83, 3174 (1999). 21, 95
[23] S. Mancini, V. I. Man'ko, and P. Tombesi, Ponderomotive control of quantum macroscopic coherence, Phys. Rev. A 55, 3042 (1997). 21
[24] S. Bose, K. Jacobs, and P. L. Knight, Preparation of nonclassical states in cavities with a moving mirror, Phys. Rev. A 56, 4175 (1997). 32, 111 129
[25] W. Marshall, C. Simon, R. Penrose, and D. Bouwmeester, Towards Quantum Superpositions of a Mirror, Phys. Rev. Lett. 91, 130401 (2003). 21, 111
[26] J. Zhang, K. Peng, and S. L. Braunstein, Quantum-state transfer from light to macroscopic oscillators, Phys. Rev. A 68, 013808 (2003). 21
[27] I. Tittonen, G. Breitenbach, T. Kalkbrenner, T. Muller, R. Conradt, S. Schiller, E. Steinsland, N. Blanc, and N. F. de Rooij, Interferometric measurements of the position of a macroscopic body: Towards observation of quantum limits, Phys. Rev. A 59, 1038 (1999). 21
[28] T. Briant, P. Cohadon, M. Pinard, and A. Heidmann, Optical phase-space reconstruction of mirror motion at the attometer level, Eur. Phys. J. D 22, 131 (2003). 64, 122
[29] O. Arcizet, P.-F. Cohadon, T. Briant, M. Pinard, A. Heidmann, J.-M. Mackowski, C. Michel, L. Pinard, O. Francais, and L. Rousseau, High-sensitivity optical monitoring of a micro-mechanical resonator with a quantum-limited optomechanical sensor, Phys. Rev. Lett. 97, 133601 (2006). 21
[31] T. Kippenberg, H. Rokhsari, T. Carmon, A. Scherer, and K. Vahala, Analysis of Radiation-Pressure Induced Mechanical Oscillation of an Optical Microcavity, Phys. Rev. Lett. 95, 033901 (2005). 21, 26
[32] S. Gigan, H. R. Bohm, M. Paternostro, F. Blaser, G. Langer, J. B. Hertzberg, K. C. Schwab, D. Bauerle, M. Aspelmeyer, and A. Zeilinger, Self-cooling of a micromirror by radiation pressure, Nature 444, 67 (2006).
[33] O. Arcizet, P.-F. Cohadon, T. Briant,M. Pinard, and A. Heidmann, Radiationpressure cooling and optomechanical instability of a micromirror, Nature 444, 71 (2006).
[34] A. Schliesser, P. Del'Haye, N. Nooshi, K. J. Vahala, and T. J. Kippenberg, Radiation Pressure Cooling of a Micromechanical Oscillator Using Dynamical Backaction, Phys. Rev. Lett. 97, 243905 (2006).
[35] T. Corbitt, Y. Chen, E. Innerhofer, H. Muller-Ebhardt, D. Ottaway, H. Rehbein, D. Sigg, S. Whitcomb, C. Wipf, and N. Mavalvala, An All-Optical Trap for a Gram-Scale Mirror, Phys. Rev. Lett. 98, 150802 (2007).
[36] S. Groblacher, S. Gigan, H. R. Bohm, A. Zeilinger, and M. Aspelmeyer,
Radiation-pressure self-cooling of a micromirror in a cryogenic environment, Europhys. Lett. 81, 54003 (2008).
[37] S. Groblacher, J. B. Hertzberg, M. R. Vanner, S. Gigan, K. C. Schwab, and M. Aspelmeyer, Demonstration of an ultracold micro-optomechanical oscillator in a cryogenic cavity, Nature Phys. 5, 485 (2009).
[38] Y.-S. Park and H. Wang, Resolved-sideband and cryogenic cooling of an optomechanical resonator, Nature
[39] T. Yamamoto, M. Neeley, E. Lucero, R. C. Bialczak, J. Kelley, M. Lenander, M. Mariantoni, A. D. O'Connell, D. Sank, H. Wang, M. Weides, J. Wenner, Y. Yin, A. N. Cleland, J. M. Martinis. Quantum process tomography of two-qubit controlled-Z and controlled-NOT gates using superconducting phase qubits. PRB 82, 184515 (2010)
[40]jauch quartz xtal theory /newline [41] Thickness Shear Mode Quartz Oscillator - Comsol
[42]Electrode configuration and elctrical dissipation of mechanical energy in quartz

crystal resontors A.j Valimaa,J.T Santos.
[43] Superconducting Cavities for Circuit Quantum Electrodynamics James Reagor.
[44] Yu-Hui Chen PHYSICAL REVIEW B 94, 075117 (2016).